

Filters With Active Tuning for Power Applications

Joshua Phinney, *Student Member, IEEE* and David J. Perreault, *Member, IEEE*

Abstract—Filters for switched-mode power converters have traditionally relied on low-pass networks—with corner frequencies well below the ripple fundamental—to attenuate switching harmonics over a range of frequencies. The filters explored in this report provide extra attenuation at *discrete* frequencies, easing the filtering requirement of accompanying low-pass networks. When a converter's switching frequency is tuned to a filter resonance using a novel phase-lock control scheme, a resonant filter can match the ripple-attenuation performance of a low-pass network for less volume, weight, and expense. The design and application of resonant filters and active-tuning control are discussed, and experimental results from the input filter and power stage of a prototype dc-dc converter are presented.

Index Terms—Active tuning, electromagnetic interference, filters, inductors, magnetic devices, phase locked loops, power conversion, resonant, resonator.

I. INTRODUCTION

LOW-PASS networks have traditionally been employed to attenuate power-converter switching ripple to acceptable levels. Ripple specifications imposed to observe conducted EMI limits or application constraints, however, can result in heavy, bulky filters which are detrimental to the transient performance of a power converter and contribute significantly to its cost. Resonant ripple filters offer attenuation comparable to low-pass networks—for less volume and weight—using the immittance peaking of parallel- and series-tuned circuits (Fig. 1) to introduce transmission nulls at discrete frequencies. Because resonant networks must typically have high Q to attenuate target harmonics sufficiently,¹ they provide only narrow-band attenuation. Operating conditions and manufacturing variations can readily cause narrow-band resonators to miss their design frequencies [2] and fail to attenuate the ripple; for this reason they are rarely employed in switching power converters.

A. Resonant Filters With Active Tuning

The filters described here circumvent this detuning problem by placing a converter's switching frequency (or a resonator's frequency response) under closed-loop control so that resonant attenuation is always maintained. In this paper we consider the case in which the switching frequency of a power converter is controlled to align with the resonant point of a filter having a se-

ries- or parallel-tuned resonance and a reduced low-pass characteristic [e.g., the buck converters of Fig. 2(a) and 2(b)]. Because the resonator effectively attenuates the ripple fundamental, an accompanying low-pass network can be designed with a higher corner frequency and smaller reactances. Inasmuch as suitably low-loss reactive components are available in a small volume, active tuning can reduce the overall size and cost of the filter network as compared to a conventional low-pass design.

Note that unlike resonant converters—which utilize the switching frequency to control the converter output—the approach described here adapts the switching frequency to best utilize the attenuation characteristics of a resonant network. Converter control can be realized with conventional pulse-width modulation (PWM) techniques, allowing the resonant-filter approach to be applied to a wide range of converter topologies. Furthermore, resonant filters with active-tuning control can process high power because they modulate a resonance or stimulus frequency to maximize the harmonic selectivity of a passive network: they do not, like active ripple filters ([3]–[5]), directly drive the waveforms they condition. Using the novel phase-lock control scheme described here, such filters can realize all the advantages of resonant networks, matching the ripple performance of low-pass filters for less volume, weight, and expense.

B. Organization of the Paper

Section II of this report introduces a simple phase-lock tuning system which controls the switching frequency of a power converter to operate at the resonant point of a filter. Section III considers the application of the phase-lock approach to the both the power stage and input filter of a buck converter. Experimental results are presented that demonstrate the value of the approach in reducing the size of passive components. Section IV considers additional applications and implementations of the phase-lock control system. Finally, conclusions are outlined in Section V.

II. PHASE-LOCK TUNING

To take advantage of high- Q resonant filters, one must ensure that the converter switching frequency remains aligned with the filter resonance across all component tolerances and operating conditions. Resonant excitation is equivalent to maintaining a resistive phase relationship (0°) between resonator voltage and current (note the impedance angles in Fig. 1). Because the phase response of a series- or parallel-tuned circuit monotonically increases or decreases around the 0° tuning point, it can be used as an error signal to control for excitation at the point of maximum immittance. The phase-lock tuning system presented in this paper employs this method precisely, feeding back the phase difference between resonator voltage and current to drive

Manuscript received October 29, 2002; revised November 1, 2002. This work was supported by the United States Office of Naval Research under ONR Grant N000140010381. Recommended by Associate Editor J. D. van Wyk.

J. Phinney is with the Laboratory for Electromagnetic and Electronic Systems, Massachusetts Institute of Technology, Cambridge, MA 02139 USA (e-mail: jphinney@mit.edu; djperrea@mit.edu).

Digital Object Identifier 10.1109/TPEL.2003.809329

¹Some high-power applications use damped, low- Q resonators precisely for their broad attenuation characteristic and insensitivity to detuning, at the expense of attenuation performance [1].

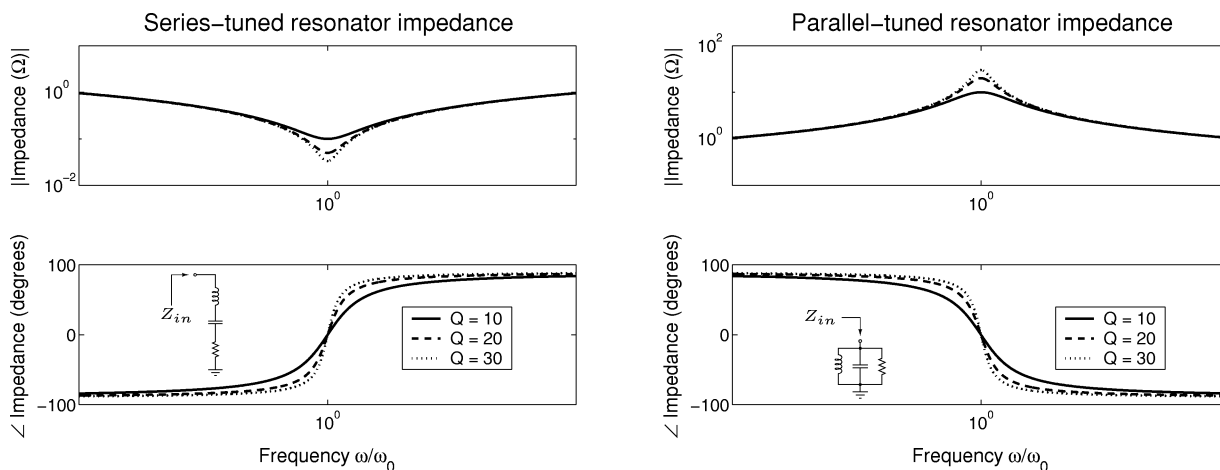


Fig. 1. Frequency response of second-order tuned circuits, normalized to the natural frequency $\omega_n = 1/\sqrt{LC}$. The impedance magnitude at a single frequency can indicate proximity to resonance (with calibration) but not whether resonance lies above or below the stimulus frequency. The impedance phase, however, increases or decreases monotonically, and its difference from 0° is an error signal indicating the distance and direction to resonance.

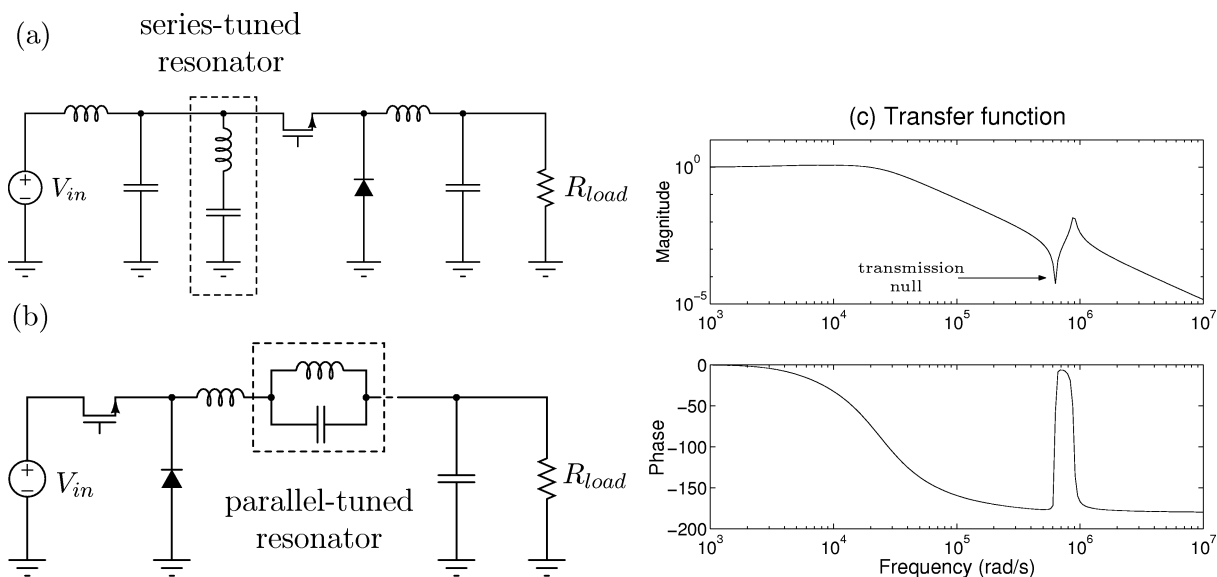


Fig. 2. Examples of a resonant filters in a buck converter. (a) The series-tuned leg provides a low-impedance current path (i.e. high attenuation) at a discrete frequency. (b) The parallel-tuned resonator presents a high impedance to switching ripple at a discrete frequency. (c) Transfer function: switch drain current to input current or switch source voltage to output voltage.

a voltage-controlled oscillator (VCO) toward the resonator’s tuned frequency.

A control topology to excite a series resonance at its minimum-impedance point is shown in Fig. 3(a). The dual of this tuning system is shown in Fig.3(b), which drives a parallel resonance at its maximum-impedance point (its resistive-impedance point). The control circuitry in either case generates the frequency command shown at the right. This command specifies the fundamental—but not the harmonic content or dc level—of the sources on the left of the block diagrams. In a power converter, the frequency command would represent an adjustable PWM frequency.

To excite the parallel- and series-tuned resonators at resonance, the controller must, in either case, adjust the fundamental drive frequency such that the resonator current and voltage *fundamentals* are in phase. The inner-loop PLL’s in Fig. 3(a) and (b) serve two functions in this regard. They provide, first of all,

a 90° phase shift in lock, which allows a subsequent phase detector (multiplier 1) to develop zero average output for a 0° V-I resonant condition in the resonators. By itself, this phase shift is poor motivation for introducing the complexity of a PLL, as the designer could employ a phase detector with 0° offset.² The more significant function of the inner-loop PLL’s, then, is to reject harmonics by locking on the *fundamental* component of an input waveform.

Consider, for example, the parallel-resonator tuning system of Fig. (3b). The differential amplifier measures the ac voltage across parallel-tuned tank, a signal with, presumably, a large fundamental component. The current through the parallel-tuned circuit, however, is dominated by its harmonic content, since the

²In fairness to an inner-loop PLL, phase detectors with 0° phase offset (state-machine detectors, typically) can be confounded by the edge timing of PWM waveforms. Signal conditioning of some sort (a filter or PLL) will probably be necessary to develop a signal with zero-crossings in phase with the fundamental component of such waveforms.

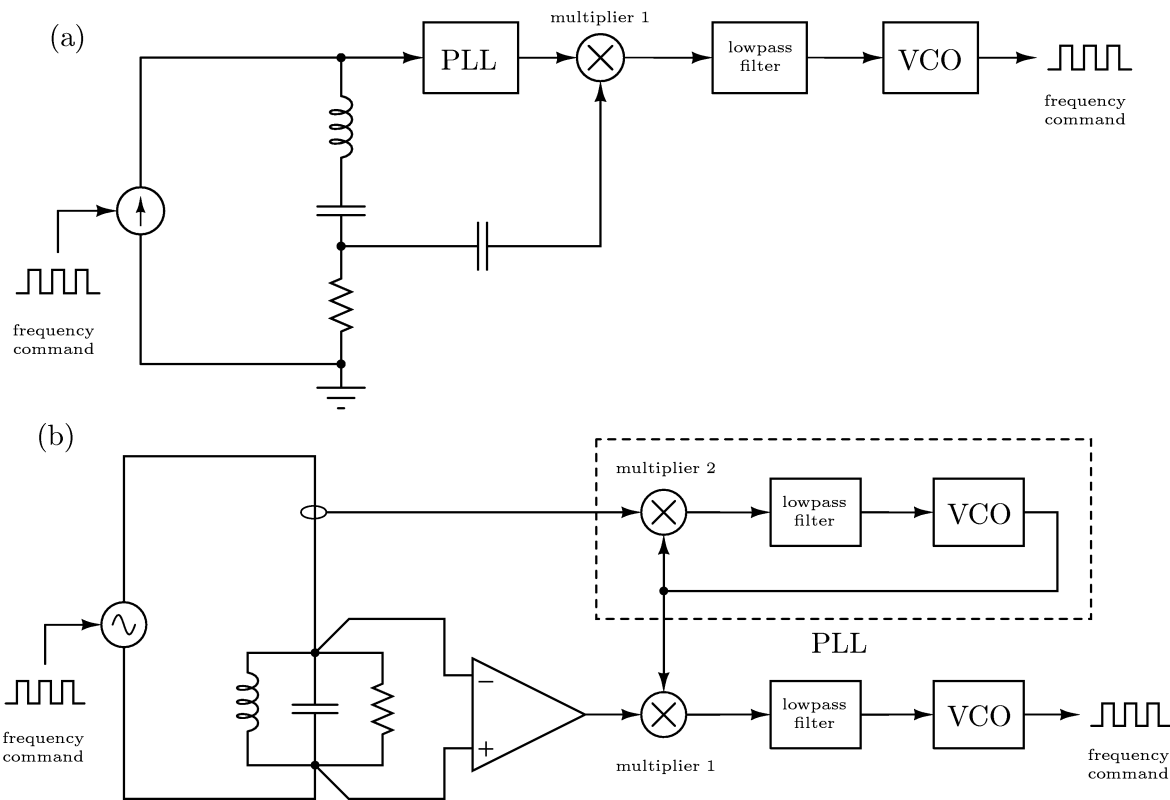


Fig. 3. Block diagram of the phase-lock tuning system for series and parallel resonators. In each case, equivalent tuning controls can be implemented by switching the sensing connections, e.g., by phase-locking to the tank voltage rather than the tank current in the lower diagram. Such an exchange, however, would not take advantage of phase-lock loop's ability to cleanly extract the fundamental component from the signal most dominated by harmonics.

resonator suppresses the fundamental inasmuch as its Q is large. The PLL effectively filters this harmonic content, extracting a signal proportional to the fundamental current only. The ac tank currents can have arbitrary harmonic content as long as the phase-lock loop employs a VCO with sinusoidal output. I.e., as long as one input of multiplier 2 is sinusoidal, the product waveform is a useful phase-detector signal when the ac tank current is *any periodic waveform* with roughly the same fundamental frequency. The low-pass PLL dynamics ensure that the multiplier develops an average detector voltage proportional to the phase error between the fundamental frequencies of its inputs: all other sum or difference frequencies are effectively attenuated. With proper selection of gains, the PLL will apply negative feedback to drive its phase error to zero, producing a *quadrature replica* of the fundamental ac resonator current even when this current is dominated by harmonics.

Multiplier 1 accepts at its inputs the phase-lock replica of the fundamental ac tank-current waveform (shifted by 90° from the original), and a measurement of the ac tank voltage. Again, only the fundamental components of the the multiplier inputs produce an average output, a product in this case proportional to the phase difference between the fundamentals of resonator voltage and current. Multiplier 1 has zero average output (zero error) for a 90° phase shift between its inputs, or zero error for a 0° V-I phase relationship at the resonator. Because of the resonator's monotonic phase slope, loop gains with the proper sign always push the outer-loop VCO (and hence the controlled ac source) toward the resonator's tuning frequency.

A. Alternative Control Topologies

It is worthwhile to pause and evaluate alternative resonant-excitation control topologies to highlight the design decisions embodied in the circuitry of Fig. 3. Consider the resonant-excitation system of Fig. 4(a). The power amplifier (the PA, which could be a switching converter or class D amplifier) drives a series-tuned resonator at the fundamental frequency commanded by the VCO, but introduces harmonics not present in the VCO output. The capacitive divider presents a high impedance to resonator currents relative to the resonator capacitance, and provides a scaled version of the resonator's internal node voltage which, at the series-resonant frequency, is a measure of the PA driving current shifted 90° . Were the PA drive purely sinusoidal, the system of Fig. 4(a) provides everything need to acquire lock: voltage and current measurements with a phase relationship at resonance corresponding to zero phase-detector error. Because the PA output voltage is harmonic-rich, however, the system does not provide a perfect measure of a phase shift between voltage and current *fundamentals*. I.e., some harmonic-current signals will appear at the capacitive-divider output, which—when multiplied by the corresponding voltage harmonics from the PA output—will produce many low-frequency product terms within the tuning system's control bandwidth. These harmonic product terms may be significant compared to the fundamental term (especially in high- Q systems), disturbing the controller's ability to maintain resonant attenuation. With aggressive filtering

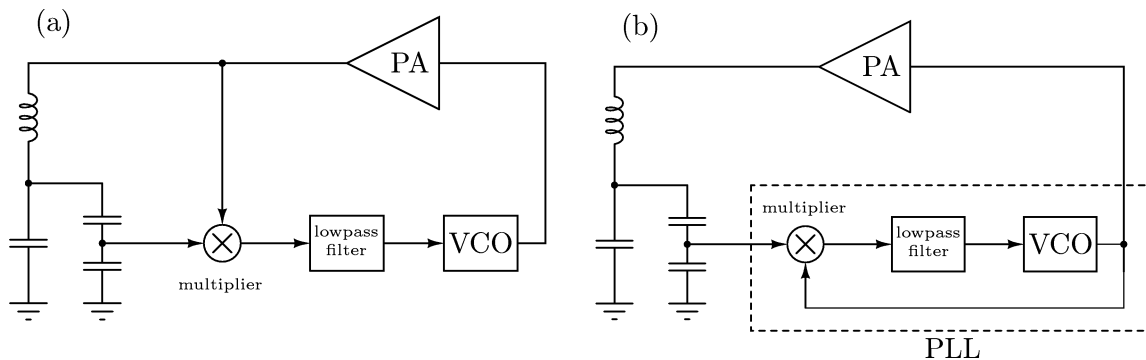


Fig. 4. Alternative resonant-excitation topologies. The PA blocks are power transimpedance amplifiers with current-drive outputs (such as switching converters). The capacitive dividers sense the current driving the series-tuned resonators (far left in each subfigure) with a 90° phase shift.

in the signal paths leading to the multiplier, though, such a tuning system might be possible. Only in systems with small power-amplifier harmonic content or low-Q resonators (see, e.g. [6]) is tuning with no special filtering feasible.

The resonance-tuning topology of Fig. 4(a) accentuates harmonic-term FM of the VCO; the scheme of Fig. 4(b) avoids this problem by multiplying the sensed current with the sinusoidal output of the VCO, eliminating all low-frequency product terms except that contributed by the V-I fundamentals. Such a design, however, is only useful when the commanded and driven phases (the phases at the input and output of the PA) are equal. For a switching power amplifier under duty-ratio control, the PA introduces duty-ratio-dependent phase shift for any $D \neq 0.5$. So, while useful for square-wave excitation of a resonance, the depicted scheme does not have the flexibility of the inner-PLL topology of Fig. 3.

B. Equivalence of Phase and Impedance Tuning Conditions

In the tank of a practical parallel-resonant filter, as suggested in Fig. 5, the inductor is the chief source of loss. In such an “almost parallel” tuned circuit, the 0° -phase frequency may be different than the maximum-impedance frequency. For inductor Q values above 10, however, these frequencies converge to within 1% of each other. Tuning for maximum impedance thus results in no appreciable phase difference between the current entering the resonator and the voltage at its terminals: the proposed control scheme can effectively maintain operation where the resonator provides maximum ripple attenuation.

C. Tuning System Dynamics

Control design for the tuning system of Fig. 3 includes design of the inner-loop PLL and design of the outer tuning loop. Among the inner-loop PLL components shown in Fig. 6 (phase detector, loop filter, and VCO), the designer typically encounters the most choices in shaping the loop filter. The loop filter, by amplifying the detector voltage v_d (itself a representation of phase error $\theta_e = \theta_i - \theta_o$), drives the VCO with a command voltage v_c away from the VCO’s average lock-frequency ω_o . Just how the loop filter uses feedback error to FM the VCO output determines most important features of PLL: its steady state frequency error, noise immunity, and lock range.

The lock range $\Delta\omega_L$ is the spread of frequencies $\pm\Delta\omega_o$ over which the PLL will acquire lock within one beat note between

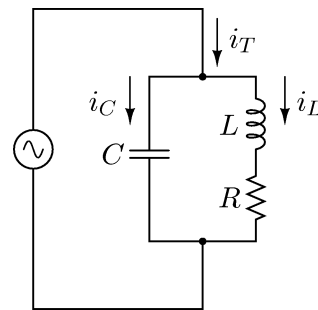


Fig. 5. “Almost-parallel” resonant circuit in which inductor loss dominates.

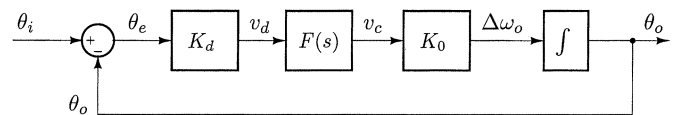
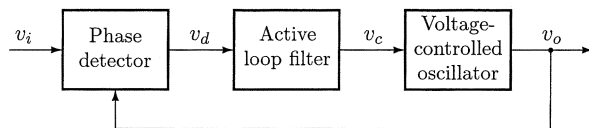


Fig. 6. Basic components of a phase-lock loop, and a linearized ac model for its locking dynamics, below, excluding phase-detector offset voltage and VCO center frequency.

the VCO and input frequency. Consider for a moment that the PLL is not locked and that the PLL input is a sinusoid at some frequency deviation $\Delta\omega_i$ away from ω_o . The multiplier detector voltage is then

$$v_d = K_d \sin(\Delta\omega_i t)$$

where the higher frequency terms are attenuated by the low-pass loop filter. The VCO command voltage is then approximately

$$v_c \approx |F(\Delta\omega_i)| \cdot K_d \sin(\Delta\omega_i t)$$

v_c is a time-varying signal which modulates the frequency of the VCO output, producing a peak frequency variation of $K_o K_d \cdot |F(\Delta\omega_i)|$. Consider the case where $\Delta\omega_i$ is greater than the VCO’s peak frequency deviation. The VCO command cannot support lock, at least not immediately, and so sweeps the VCO output at the beat note frequency $\Delta\omega_i$. If ω_i is brought closer to ω_o , so that $\Delta\omega_o$ just equals $K_o K_d \cdot |F(\Delta\omega_i)|$, v_c is able to

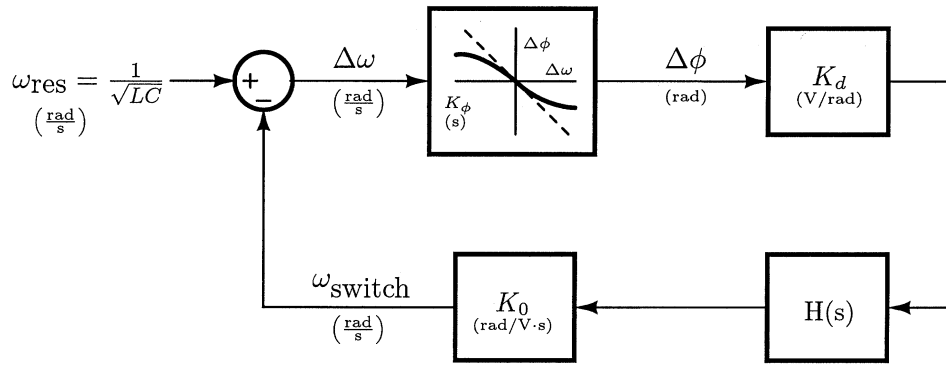


Fig. 7. Linearized model for the phase-sensing tuning system in lock.

support the lock condition $\omega_i = \omega_o$ at the extreme edge of its modulation range. $\Delta\omega_L$ is therefore determined approximately by the nonlinear equation

$$\Delta\omega_L \approx K_o D_d \cdot |F(\Delta\omega_L)|.$$

Through some simplifying approximations for $|F(\Delta\omega_L)|$, the lock range for a PI filter (like that shown in Fig. 8) in a high gain loop is $\Delta\omega_L \approx 2\zeta\omega_n$, and the PLL's closed-loop phase transfer function is

$$T(s) = \frac{2s\zeta\omega_n + \omega_n^2}{s^2 + 2s\zeta\omega_n + \omega_n^2}$$

with $\omega_n = \sqrt{\frac{K_0 K_d}{\tau_1}}$ and $\zeta = \frac{\omega_n \tau_2}{2}$.

An additional high-frequency pole in $F(s)$ (provided by C_1 and C_3 in Fig. 8) is typically added to the loop filter—far enough beyond crossover to effect the locking dynamics only slightly—to improve PLL noise immunity. Modeling and design of linear PLL's with multiplier phase detectors is further developed in many sources, including [7]–[9].

Fig. 7 shows a linear model for the tuning system dynamics in lock. The ω_{res} reference is the 0° V-I tuning frequency of the resonant filter. This reference can vary from resonator to resonator due to component tolerances, and can experience abrupt changes during load-step inductance swings. The K_ϕ block represents the fundamental-frequency phase-sensing action of the inner-loop PLL. When the inner-loop PLL dynamics are fast compared to the overall tuning dynamics, phase-shift sensing—i.e. the generation of a quadrature replica of resonator voltage or current, and the operation of the outer-loop phase detector—can be represented algebraically. K_ϕ is then just the small-signal phase gain of the resonator, the incremental change in phase-shift for an excursion $\Delta\omega$ of the switching frequency away from ω_{res}

$$K_\phi = \frac{d}{d\omega} \left[\tan^{-1} \left(\frac{\frac{\omega R}{L}}{\frac{1}{LC} - \omega^2} \right) \right] \Big|_{\omega=\omega_{res}}$$

$$K_\phi = \frac{-\frac{R}{L} \left(\frac{1}{LC} + \omega^2 \right)}{\left(\frac{1}{LC} - \omega^2 \right)^2 + \left(\frac{\omega R}{L} \right)^2} \Big|_{\omega=\omega_{res}}$$

$$K_\phi = -\frac{2L}{R} = -\frac{2}{\omega_{res}^2 RC} = -\frac{2Q}{\omega_{res}}$$

The three remaining blocks, K_d , K_o , and $H(s)$ are identical to their counterparts in the linearized model of the basic PLL (see, for instance, [8]). K_d is the phase-detector gain, the average phase-detector voltage developed per radian phase deviation in the locked condition. K_o is the VCO gain, a measure of the change in VCO frequency for a change in VCO command voltage. $H(s)$ is a loop-shaping filter which, in the prototype systems, contains an integrator to support the VCO command with zero steady-state frequency error, and a low-frequency pole to further limit the bandwidth of phase-error signals from the outer-loop multiplier. Note that no integrator is required in the “nested-PLL” model because the tuning system does not operate on phase signals, but aligns frequencies. The output of the K_0 block, the converter frequency command, can sustain arbitrary phase shift (e.g., from converter dynamics) without affecting the operation of the tuning system. A more detailed view of the frequency-tuning circuitry used in the prototype systems is shown in Fig. 8, with important component values given in Table I.

Though the block diagram of Fig. 7 has proven satisfactory for developing tuning controls, it does not indicate all details relevant to locking and hold-in performance. In particular, the K_ϕ block summarizes the result of multiplications involving two sensed signals, each of which is a potential source of destabilizing disturbances. Though it is difficult to determine whether the performance of the system depicted in Fig. 7 is limited by the inner loop, the tuning controller exhibits the locking and hold-in trade-off typical of a simple PLL. I.e., choice of a narrow outer-loop bandwidth has been observed to *prevent* (not just slow) the tuning process, as might be expected for PLL pull-in acquisition of a noisy signal. The converter ripple waveforms sensed by the tuning controller can be small signals (<10 mV) with large ringing voltages around switch transitions. Though the noise theory of the PLL (a cumbersome topic) has not been extended to guide the selection of outer-loop bandwidth, we have been able to develop tuning controllers that reliably achieved resonance lock in under one second using the presented model.

III. APPLICATION TO A DC-DC CONVERTER

To demonstrate the advantages of controlled resonant filtering, a tuned-filter approach was applied in the design of both a power stage and input filter for a 12-V output, 300 W buck converter. In each case, a filter network comprising a

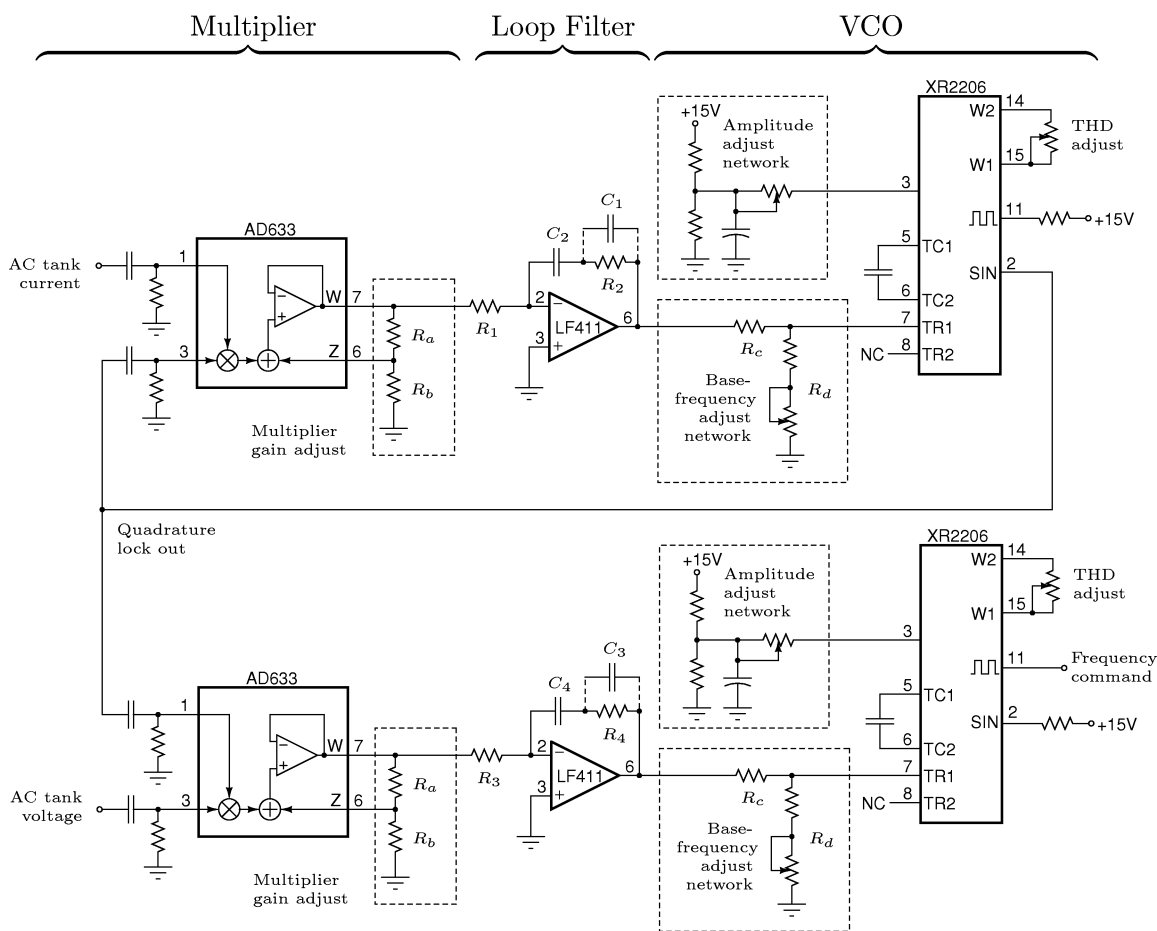


Fig. 8. Schematic of the inner-loop PLL and outer-loop tuning controller used in the prototype system.

TABLE I
COMPONENT VALUES FOR THE SCHEMATIC OF FIG. 8

R_a	1 k Ω	phase-detector gain adjust
R_b	100 k Ω	phase-detector gain adjust
C_2, C_4	0.22 μ F	compensation
C_1, C_3	0.01 μ F	compensation
R_2, R_4	68 k Ω	compensation
R_1, R_3	180 k Ω	compensation
C_T	0.0022 μ F	XR2206 timing (pins 5 and 6)
R_c	75 k Ω	VCO base freq. adjust
R_d	4.7 k Ω + 1 k Ω pot	VCO base freq. adjust

parallel-tuned resonator in series with an inductor replaced a single inductor.

A. Resonant Power-Stage Filter

Fig. 9 shows a block diagram of the prototype buck converter incorporating a resonant power-stage network and active-tuning controls. Tuning is necessary for the high-Q filter designs that exhibit the best performance subject to a limit on total inductor size. 200 μ H total inductance—measured at highest saturation—was chosen to limit the size of a resonant filter in the first example converter. This total inductance was split between

a low-pass inductor and a resonant inductor (Fig. 10) in the proportion that produced the smallest output current ripple over a duty-ratio range of interest. All inductors were designed to minimize the volume of single-wound, powdered-iron toroids under worst-case operating conditions, i.e. full dc magnetizing force and highest peak-peak ac flux density. Optimization resulted in $L_1 = 235 \mu$ H and $L_2 = 127 \mu$ H at 0% saturation. A small polypropylene capacitor $C(0.033 \mu$ F) was chosen to resonate with L_2 near 100 kHz, and produced tuning points in the range of 108–131 kHz as L_2 saturated under increasing dc bias. For comparison, a conventional single series inductance L_3 was designed to achieve equivalent ripple performance over the chosen duty-ratio range, resulting in $L_3 = 1.14$ mH at 0% saturation.

The control design focused on achieving stable, reliable locking of the converter switching frequency on the filter resonant point. See [7]–[9] for a discussion of the modeling and design of the linear PLL of Figs. 3 and 9. An active proportional + integral (PI) loop filter was chosen to minimize steady-state phase error, and the PLL bandwidth was selected such that its lock-in range covered the expected range of resonant frequencies (see schematic, Fig. 8). The linearized tuning dynamics of the outer loop (Fig. 7) exhibit the same lock-in and holding performance trade-offs as the linear PLL. I.e., lower outer-loop bandwidth decreases phase jitter and improves lock-in reliability at the expense of lower lock range,

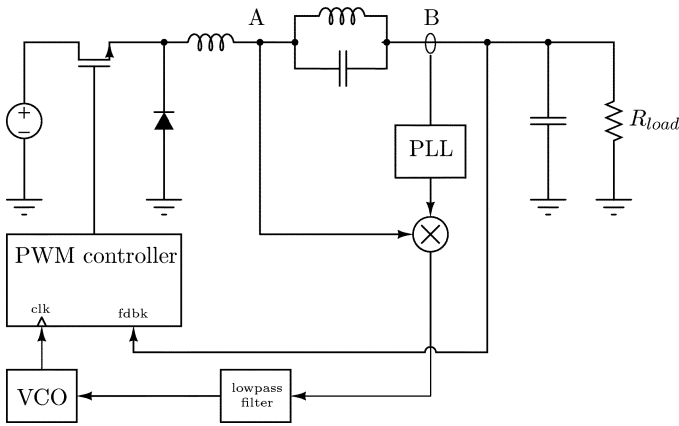


Fig. 9. Block diagram of phase-lock tuning system used to align a buck converter's switching frequency to the maximum-impedance resonance of its output filter. A ground-referenced voltage measurement is made at point A, from which the AC voltage across the tank is determined. The resonator current is measured at point B.

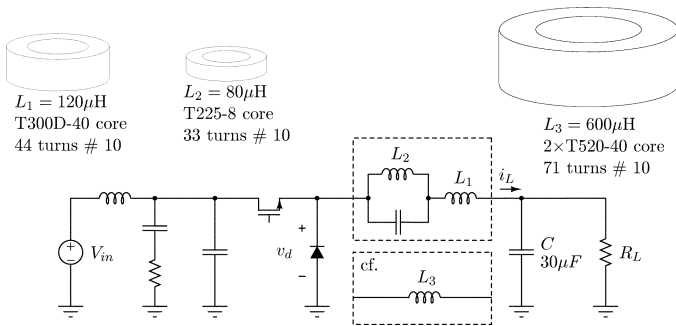


Fig. 10. Comparison of the core sizes for the power stage of a 300 W buck converter.

whereas large bandwidth extends lock range at the expense of holding performance. The switching currents of the converter power stage can be a significant source of noise power, and large loop bandwidths can cause the tuning system to lose lock. We demonstrated that the system functioned reliably, however, without the special pull-in techniques often required for noisy signals.

As seen from the measured current ripple in Fig. 12, both the resonant power stage and single buck inductor meet a challenging 120 mA maximum-ripple-current specification for all duty ratios greater than 0.38. The applied ripple fundamental has the largest magnitude at $D = 0.5$, around which point the resonant filter obtains the greatest benefit from its parallel-tuned network and outperforms the single inductor at each duty ratio in the range $0.38 < D < 0.62$. The resonant network with active tuning achieves this performance for 3.7 times less total filter volume (151 cm^3 compared to 557 cm^3) and 3.6 times less total filter mass (691 g compared to 2500 g) than the conventional single inductor. The conventional filter inductor necessary to match the performance of the resonant filter is impractically large. The resonant filter is of acceptable size, and enables operation at lower ripple ratios than might otherwise be practical.

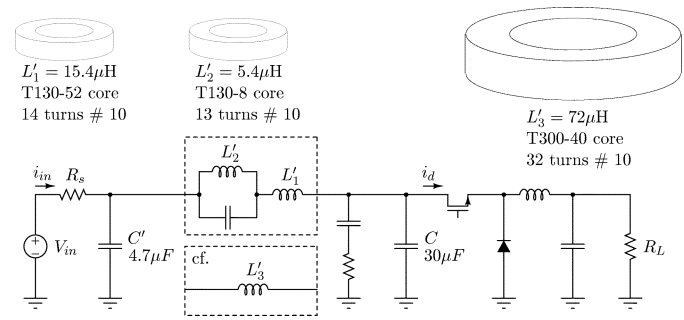


Fig. 11. Comparison of the core sizes for the input filter of a 300 W buck converter. The small film capacitors did not contribute significantly to the filter volume.

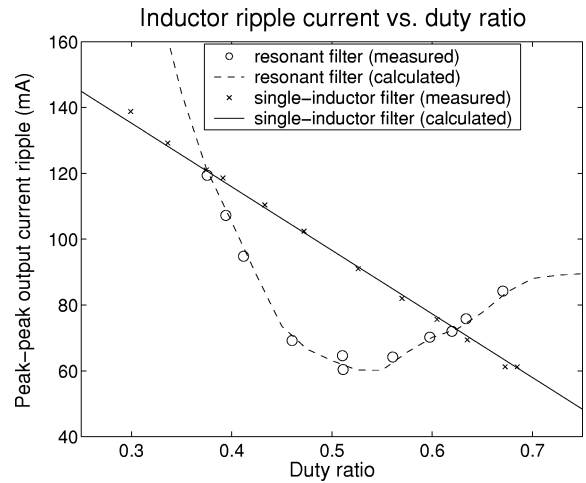


Fig. 12. Comparison of the peak-peak inductor ripple current performance of the single-inductor and resonant power stages.

B. Operation at Higher Ripple Ratios

Deep continuous conduction—or, equivalently, low ripple ratios—favor resonant filters. Circulating tank currents are Q times larger than ripple currents at the resonator terminals, and can produce large peak ac flux density (hence high loss) in a resonant inductor. Should the designer choose to operate with higher power-stage ripple, a resonant inductor using the same core material may have to be made larger to support circulating currents with acceptable Q . To assess the performance of resonant filters at higher ripple ratios, a family of 300 kHz, 36 W resonant converters were simulated. Several hundred passive designs, using various combinations of Coilcraft SMT inductors ([10]), were scrutinized, and two representative designs at the frontiers of performance were constructed and tested. For each converter, a phasor analysis program calculated current waveforms in each inductor, and designs were discarded which drove either peak current above saturation limits or RMS current above the manufacturer's 40°C -rise limits. The phasor analysis applied to all harmonics the ac resistance measured at the switching frequency, and made no more sophisticated account of skin effect or core loss.

Results of this study are illustrated in Fig. 13. Fig. 13(a) compares the filter volume of resonant and nonresonant filters across ripple ratio. For designs with low ripple ratio (i.e., less than 20%), significant improvement in filter volume is obtained.

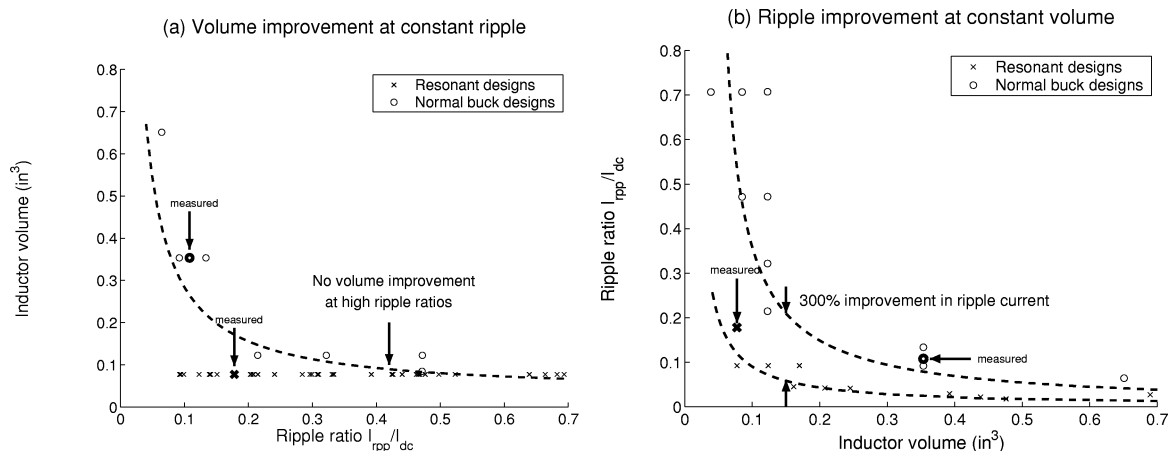


Fig. 13. Comparison of resonant and nonresonant buck converter magnetics designs. (a) Presentation comparing volume over peak-peak inductor current levels, including high ripple ratios which favor nonresonant designs. (b) Presentation comparing ripple ratio when resonant and nonresonant magnetics are allowed to fill the same volume.

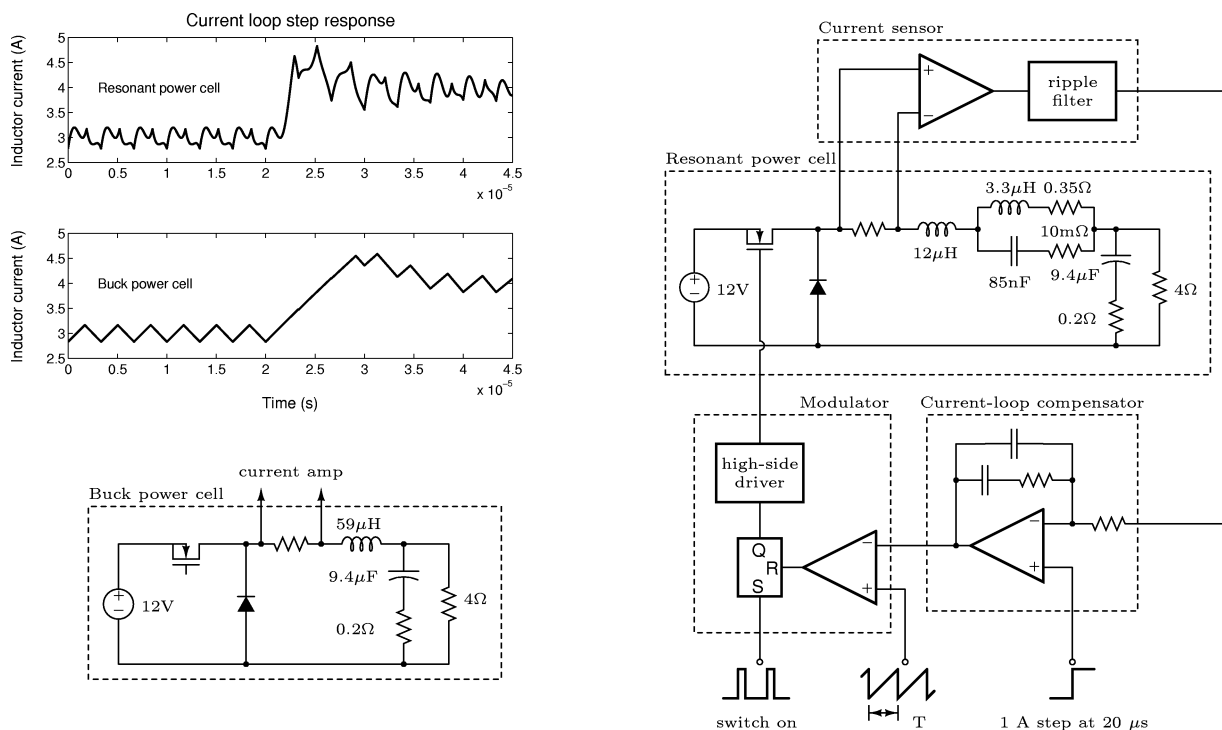


Fig. 14. Circuits and current-loop step responses for the buck and resonant power cells under average current-mode control. The compensators were designed based on a maximum slope provided to the modulator. The converter with the resonant filter has an average inductor-current rise-time more than twice as fast as the regular buck converter, for the same phase margin and ripple performance.

As the ripple ratio approaches 40%, no volume improvement is achieved, though resonant networks offer a potential control-bandwidth improvement. At even higher ripple current, resonators must become larger than simple buck inductors to sustain large circulating current with adequate Q .

Fig. 13(b) compares ripple performance as a function of filter volume for resonant and nonresonant filter designs. As can be seen from the trends in the best-performing designs, resonant filter networks offer approximately a factor of three improvement in ripple performance over conventional filters for any given filter volume. Note that if efficiency is of particular con-

cern, a resonant network allows a designer to lower switching frequency and switching loss without sacrificing ripple performance or filter volume.

C. Control of Resonant Power Cells

The reduction of total filter inductance in the resonant filter (cf. L_3 compared to the combination of L_1 and L_2 in Fig. 10) also improves converter control characteristics. The resonant network provides the attenuation performance of a large inductance (L_3), while presenting an inductance about three times smaller ($L_1 + L_2$) at control frequencies ($\ll f_{sw}$). This smaller

reactance permits more rapid transient response (e.g. to load steps) than is conventionally possible at low ripple ratios.³

Consider Fig. 14, detailing simulations of 300 kHz, 36 W buck converters (both ferrite, resonant and nonresonant) under average current-mode control. The current ripple filter was required in the resonant-filter controller (but not the single-inductor converter) to amplify the ripple fundamental with respect to its harmonics. Without this precaution, third-harmonic ripple inflections greatly complicated transient behavior of the averaged dynamics. The compensators were designed based on a maximum output slope provided to the modulator, with low frequency gain added for good tracking and roll-off around the switching frequency [11]. The compensator transfer functions $G_c(s)$ used were

$$278 \times 10^3 \cdot \frac{\frac{s}{188.4 \times 10^3} + 1}{s \left(\frac{1}{1.88 \times 10^6} + 1 \right)} \quad \text{nonresonant}$$

$$94.2 \times 10^3 \cdot \frac{\frac{s}{188.4 \times 10^3} + 1}{s \left(\frac{1}{5.65 \times 10^6} + 1 \right)} \quad \text{resonant.}$$

The converter with the resonant filter has an average-inductor-current rise time more than twice as fast as the regular buck converter, for the same phase margin and ripple performance (at $D = 0.5$). The power-cell resonance is closed within the current loop, so the outer voltage-loop has no special complications: the controller commands inductor current into the same load and output capacitor, but with higher bandwidth in the resonant case. That the resonant filter behaves like a smaller inductor across its regulation bandwidth is plausible: the resonator Q is high enough so that impedance variations are appreciable only above half the switching frequency, yet not so high that earlier crossover is necessary to maintain acceptable gain margin.

D. Resonant Input Filter

The low ripple ratios that are most favorable for resonant filters are common in input and output filters for switching converters. In such applications, resonant networks offer clear volume and mass savings. To demonstrate this improvement, both conventional and resonant input filters were developed for the prototype 300 W, 12 V converter. Consider the conventional and resonant input filters of Fig. 11. The AC currents measured through L'_1 and L'_3 , respectively, are plotted in Fig. 15 as a function of duty ratio. The resonant and low-pass networks have essentially identical performance and, when incorporated in a π -section filter with a capacitance C' across a 50Ω source impedance (at ripple frequencies), meet a flat $-90 \text{ dB}\mu\text{V}$ ripple specification. The resonant filter matches the performance of the conventional design with 92 g and 19 cm^3 , 3.0 times less total filter volume and 2.8 times less mass than with L_3 alone.

E. Summary

As these example show, resonant filters and active tuning can provide substantial advantages in converter power stages and

³Faster converter response is compatible with voltage-mode or average-current-mode control. Control schemes which focus on converter waveforms at ripple frequencies (e.g., peak current-mode control or hysteretic current control) cannot be applied in any obvious manner to resonant filters.

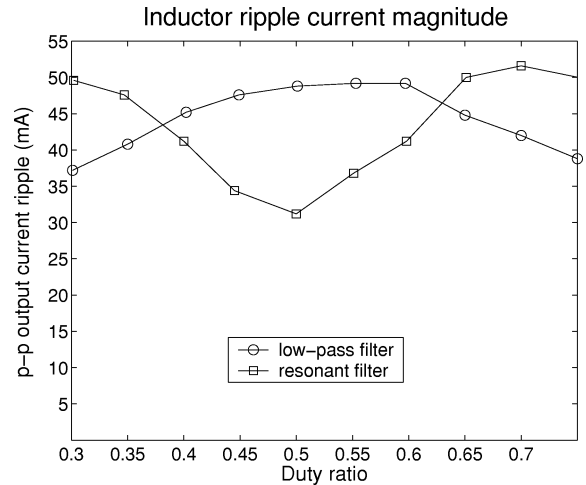


Fig. 15. Comparison of the peak-peak ripple performance of the single-inductor and resonant input filters.

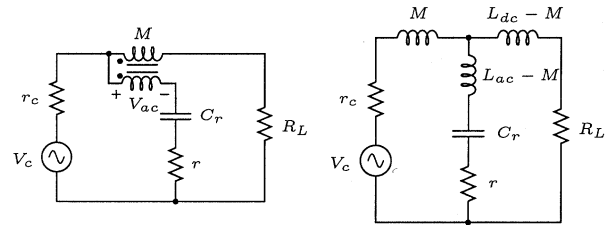


Fig. 16. Magnetically coupled shunt resonator and its equivalent T model, excited by a voltage source V_c representing the switch source node or output of a switching converter.

in input and output filters. The designer can use this approach to greatly reduce the size of filter components, or achieve improved ripple performance for a given filter size. Alternatively, a given filter size can support—with resonant techniques—a much lower switching frequency with constant ripple performance, thus realizing a substantial improvement in efficiency. While the resonant approach has been demonstrated for a simple buck converter, it is directly applicable to the a wide range of power converter topologies (e.g., Fig. 17) and fixed-frequency control methods.

IV. ALTERNATIVE APPLICATIONS AND IMPLEMENTATIONS

A. Shunt Resonant Filters

The above tuning method is a general technique for controlling the phase relationship of signals, and can be applied to series- and parallel-tuned circuits in the power stages (Figs. 2, 17), input filters (Fig. 11), or output filters of switching converters. Filters containing series-tuned shunt resonators and magnetically coupled shunt resonators (Figs. 2(b) and 16] were also considered for use in conjunction with the phase-lock tuning system. Shunt networks divert ripple current by presenting low ac impedance at the switching frequency and its harmonics. The impedance magnitude of a series-tuned network at its resonant point, not its Q, is therefore the metric of resonator performance. As a result, it is not clear that a high-Q design (one in need of tuning control) will provide the best

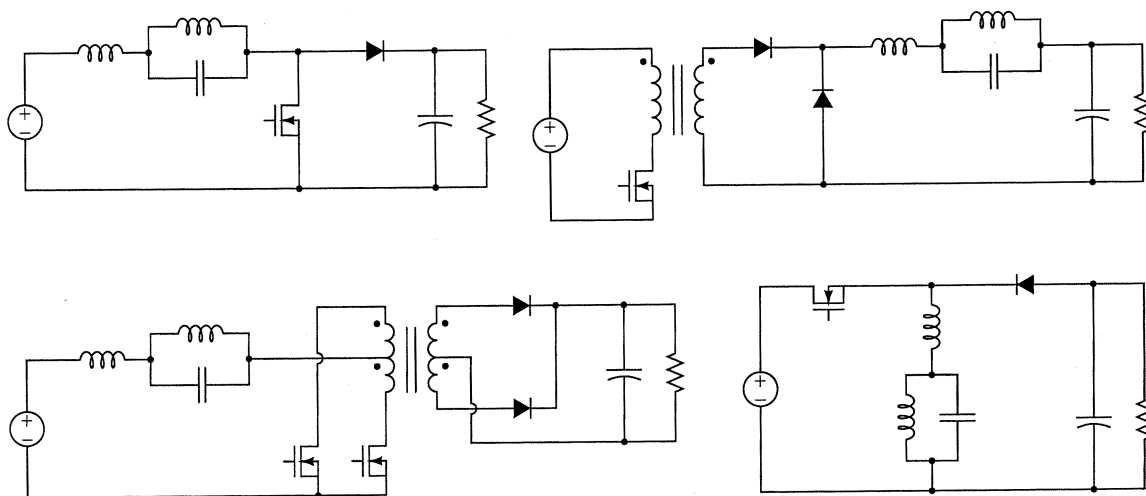


Fig. 17. Parallel-tuned resonant filters can be applied to the power stages of most major PWM switching-converter topologies.

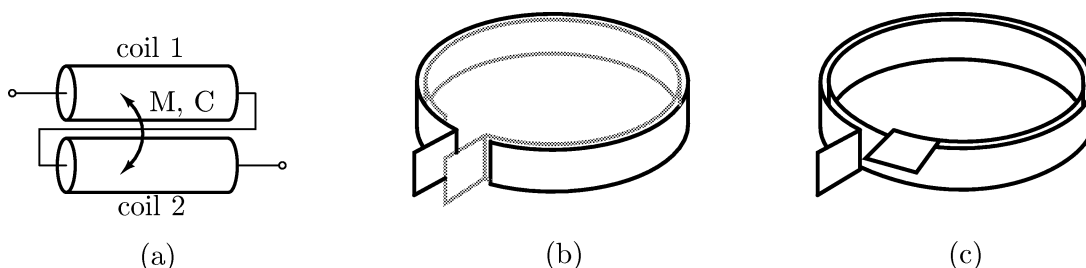


Fig. 18. Hybrid inductive-capacitive elements that exhibit resonances: (a) and (c) self-resonant inductors with large inter-turn or inter-coil capacitance and (b) schematic depiction of a resonant foil capacitor, similar to a typical film capacitor without extended-foil contacts.

filtering performance.⁴ The best shunt resonator—the resonator with the lowest possible characteristic impedance—is often just the largest possible capacitor, self-resonant at a frequency of particular interest. Applications in which the allowed capacitor size is limited, or those which can take advantage of the intrinsic inductance of available capacitors, could benefit from series-resonant filters.

B. Resonant Components

Phase-lock tuning can realize the benefits of such resonant structures that, like the lumped resonator in the example filter, are otherwise limited by component tolerances. Single-resonant [12] and multiresonant [13] inductors, for instance, use magnetically coupled tuned circuits to produce high impedances at discrete frequencies. Such structures exploit mutual inductance and inter-winding capacitance [M and C in Fig. 18(a)] between coils to introduce impedance peaks at one or more frequencies. Additional coils that do not carry dc current can be magnetically coupled to the principle winding, and two-terminal devices with as many as three resonances have been demonstrated in [13].

The self-resonant capacitor/inductor hybrids of [14]–[18], are wound-foil structures which exhibit repeatable resonances with

⁴Note that Q can be made arbitrarily high by increasing a resonator's characteristic impedance with inductor-heavy designs: ESR rises more slowly than inductance, so that Q increases, but ESR still increases. This performance trend is fundamentally opposed to the need for tuning, as the lowest-ESR design spoils series-tuned Q .

low loss. Schematically, these hybrid structures introduce controlled self-inductance in galvanically isolated foil turns [Fig. 18(b)] to implement a series-resonant capacitor, or introduce controlled inter-turn capacitance in a single foil strip [Fig. 18(c)] to produce a parallel-resonant inductor. Such structures can have particularly low loss (a 170 kHz Q of 155 is reported in [18]) because of the low-impedance foil construction and the use of the same conductor for both magnetic and electric storage. Shunt resonators, which for discrete passives were found to be unacceptably lossy in the design example, may perhaps be implemented inexpensively with good performance using such hybrid passive elements.

Variations in driving circuitry, manufactured geometry, and temperature (and, importantly, dc magnetizing force and ac flux density when magnetic materials are present) can alter the tuning point of all these resonant structures to such a degree that their filtering properties may be of little benefit in a practical system without tuning. Moreover, distributed models or high-order finite-dimensional approximations are required, in the case of foil resonators at least, to predict resonant frequencies. With active-tuning control for *excitation at resonance*, the full filtering benefits of the above-mentioned structures can be practically realized with minimal design effort. Though not employed for filtering, core-less planar transformers [19] and core-less twisted-coil transformers [20] exhibit maximum-efficiency points characterized by resistive V-I phase relationships at their ports. Effective use of such

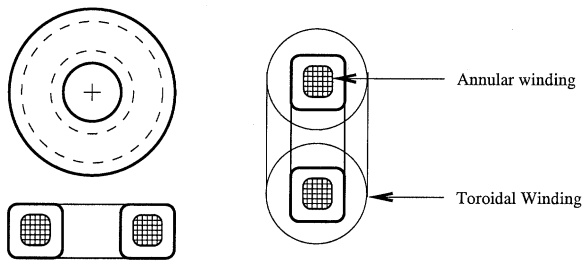


Fig. 19. Structural diagram of a cross-field reactor. The magnetic core is wound with two windings (an annular coil and a toroidal coil) that are not coupled in the usual sense. Current in one winding modulates the inductance seen at the other winding.

structures, likewise, is a task ideally suited to phase-sensing control.

C. Resonance Tuning

Phase-sensing control can be applied to tune a filter resonant frequency rather than a converter switching frequency. For instance, an electrically controlled reactance implemented with a cross-field reactor (Fig. 19, and see [21]–[23]) can shift a filter transmission null as currents are applied to its control winding. A nested PLL topology like that presented for the frequency tuning case can excite the network containing the cross-field reactor to achieve controlled operation at resonance. An advantage of the resonance-tuning approach is that it can support tuned attenuation of multiple frequencies using multiple resonant networks. Magnetic tuning may also be valuable in coupled-inductor filters and ripple-current steering structures ([24]–[27]) where control of coupling can improve performance.

V. CONCLUSION

By modulating a switching frequency or filter resonance to maximize a resonant-network impedance, phase-lock tuning makes practical the inclusion of narrow-band resonators in passive ripple filters. Filters with active tuning offset resonant-point variations caused by manufacturing tolerances and fluctuating operating conditions, and so can realize—repeatedly and without compromised ripple performance—the size and weight decreases possible with resonant networks and magnetic structures. As demonstrated by the power stage and input filter designs in the prototype converters, a tuned filter can meet the same ripple specification as a conventional design with only one-third the mass and volume, for low ripple ratios. A resonant design can always provide lower ripple ratios for a given filter volume.

The phase-lock resonant-excitation technique requires an additional control loop, but no additional power-processing devices in its frequency-modulating form. PWM controller ICs could be augmented to accept voltage- and current-ripple waveforms with as few as two pins (for ground-referenced signals). The remaining control elements—multipliers, signal filters, and VCOs—are integrable with no external connections if the loop-filter bandwidths are predetermined. The lighter and less bulky reactive components of actively tuned filters certainly justify this extra control circuitry whenever power quality and converter size and weight are top priorities.

REFERENCES

- [1] S. D. Upadhye and Y. R. Atre, "Determination of the design parameters of passive harmonic filters using nonlinear optimization," in *Proc. 1998 IEEE Ind. Comm. Power Syst. Tech. Conf.*, 1998, pp. 155–164.
- [2] K. P. Lin, M. H. Lin, and T. P. Lin, "An advanced computer code for single-tuned harmonic filter design," *IEEE Trans. Ind. Applicat.*, vol. 34, no. 4, pp. 640–648, July/Aug. 1998.
- [3] M. Zhu, D. J. Perreault, V. Caliskan, T. C. Neugebauer, S. Guttowski, and J. G. Kassakian, "Design and evaluation of an active ripple filter with Rogoski-coil current sensing," in *Proc. IEEE Power Electron. Spec. Conf.*, 1999, pp. 874–880.
- [4] L. E. LaWhite and M. F. Schlecht, "Active filters for 1-MHz power circuits with strict input/output ripple requirements," *IEEE Trans. Power Electron.*, vol. PE-2, pp. 282–290, May 1994.
- [5] N. K. Poon *et al.*, "Techniques for input ripple current cancellation: classification and implementation," *IEEE Trans. Power Electron.*, vol. 15, pp. 1144–1152, Nov 2000.
- [6] D. L. Logue, "Power electronic building block application in optimization, control, and synthesis," Ph.D. thesis, Dept. of Elect. Comput. Eng., Univ. of Illinois, Urbana, IL, 2000.
- [7] R. E. Best, *Phase-Locked Loops*, 3rd ed. New York: McGraw-Hill, 1997.
- [8] D. H. Wolaver, *Phase-Locked Loop Circuit Design*. Englewood Cliffs, New Jersey: Prentice-Hall, 1991.
- [9] J. W. Phinney, "Filters with Active Tuning for Power Applications," S.M. thesis, Dept. of Elect. Comput. Eng., Mass. Inst. of Technol., Lab. Electromagn. Electron. Syst., Cambridge, MA, 2001.
- [10] Coilcraft, *Inductors, Transformers, and Filters Catalog*, Aug. 2000.
- [11] L. Dixon, "Average current mode control of switching power supplies," *Unitrode Applicat. U-140*, 1999.
- [12] Y. Midorikawa, S. Hayano, and Y. Saito, "A new inductor having noise-filtering capability," *IEEE Trans. Magn.*, vol. 30, pp. 4761–4763, Nov. 1994.
- [13] Y. Midorikawa, S. Hayano, and Y. Saito, "A multi-resonant type inductor having notch-filtering capability," *IEEE Trans. Magn.*, vol. 32, pp. 4998–5000, Sept. 1996.
- [14] R. J. Kemp, P. N. Murgatroyd, and N. J. Walker, "Self-resonance in foil inductors," *Electronics Letters*, vol. 11, no. 15, pp. 337–338, July, 24th 1975.
- [15] R. Reeves, "Inductor-capacitor hybrid," in *Proc. Inst. Elect. Eng.*, vol. 122, Nov. 1975, pp. 1323–1326.
- [16] P. N. Murgatroyd and N. J. Walker, "Lumped-circuit model for inductor-capacitor hybrid," *Electron. Lett.*, vol. 12, pp. 2–3, Jan. 1976.
- [17] R. Reeves, "Choke-capacitor hybrid as a fluorescent-lamp ballast," in *Proc. Inst. Elect. Eng.*, vol. 122, Oct. 1975, pp. 1151–1152.
- [18] M. Ehsani, O. H. Stielau, and J. D. van Wyk, "Integrated reactive components in power electronic circuits," *IEEE Trans. Power Electron.*, vol. 8, pp. 208–215, Apr. 1993.
- [19] S. C. Tang, S. Y. R. Hui, and H. S.-H. Chung, "Coreless planar printed-circuit-board (PCB) transformers—a fundamental concept for signal and energy transfer," *IEEE Trans. Power Electron.*, vol. 15, pp. 931–941, Sept. 2000.
- [20] S. Hayano, Y. Nakajima, H. Saotome, and Y. Saito, "A new type high-frequency transformer [sic]," *IEEE Trans. Magn.*, vol. 27, pp. 5205–5207, Nov. 1991.
- [21] R. Hertz and H. Buelteman, "The application of perpendicularly superposed magnetic fields," *AIEE Trans.*, vol. 74, pp. 655–660, Nov. 1955.
- [22] H. J. McCreary, "The magnetic cross valve," *AIEE Trans.*, vol. 70, no. 2, pp. 1868–1875, 1951.
- [23] F. J. Beck and J. M. Kelly, "Magnetization in perpendicularly superposed direct and alternating fields," *J. Appl. Phys.*, vol. 19, pp. 551–562, June 1948.
- [24] S. Cuk, "A new zero-ripple switching dc-dc converter and integrated magnetics," *IEEE Trans. Magn.*, vol. MAG-19, pp. 57–75, Mar. 1983.
- [25] S. Senini and P. Wolfs, "The coupled inductor filter: analysis and design for ac systems," *IEEE Trans. Ind. Electron.*, vol. 45, pp. 574–578, Aug. 1998.
- [26] G. Bloom and R. Severns, "The generalized use of integrated magnetics and zero-ripple techniques in switchmode power converters," *IEEE Power Electron. Spec. Conf.*, pp. 15–13, 1984.
- [27] S. Feng, W. Sander III, and T. Wilson, "Small-capacitance nondissipative ripple filters for DC supplies," *IEEE Trans. Magn.*, vol. MAG-6, pp. 137–142, Mar. 1970.

- [28] J. G. Kassakian, M. F. Schlecht, and G. C. Verghese, *Principles of Power Electronics*. New York: Addison-Wesley, 1991.
- [29] T. K. Phelps and W. S. Tate, "Optimizing passive input filter design," in *Proc. Powercon 6*, May 1979, pp. G1-1–G1-10.



Joshua W. Phinney (S'97) received the B.S. degree from the University of Illinois at Chicago in 1999, and the S.M. degree from the Massachusetts Institute of Technology, Cambridge, in 2001, both in electrical engineering.

He is currently a Research Assistant in the Laboratory for Electromagnetic and Electronic Systems, Massachusetts Institute of Technology, where his research interests include the design and control of miniaturized power converters, power MEMS, and hybrid passive components.



David J. Perreault (S'91–M'97) was born in North Providence, RI, on January 22, 1967. He received the B.S. degree in electrical engineering from Boston University, Boston, MA, in 1989, and the S.M. and Ph.D. degrees in electrical engineering from the Massachusetts Institute of Technology (MIT), Cambridge, in 1991 and 1997, respectively.

He is currently an Assistant Professor with the Department of Electrical Engineering and Computer Science, MIT, and is affiliated with the Laboratory for Electromagnetic and Electronic Systems, MIT, where his work includes the investigation of new methods for the design and control of power-electronic systems.

Dr. Perreault received the Office of Naval Research's Young Investigator Program Award in 2002. He is a member of Tau Beta Pi, Sigma Xi, and the National Society of Professional Engineers.